

LBL-7284 C. 2  
UC-37

RECEIVED  
LAWRENCE  
BERKELEY LABORATORY

APR 24 1979

LIBRARY AND  
DOCUMENTS SECTION

THE APPLICATION OF X-RAY EMISSION SPECTRA TO THE  
IDENTIFICATION OF PARTICULATE SULFUR COMPOUNDS IN AMBIENT AIR

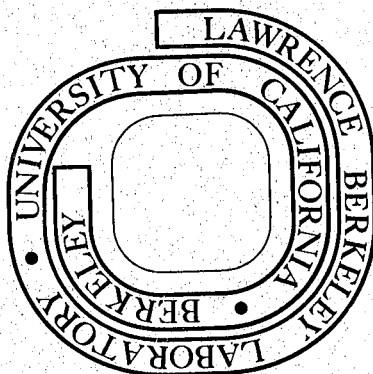
A. J. Ramponi and J. M. Jaklevic

December 1978

Prepared for the U. S. Department of Energy  
under Contract W-7405-ENG-48

**TWO-WEEK LOAN COPY**

*This is a Library Circulating Copy  
which may be borrowed for two weeks.  
For a personal retention copy, call  
Tech. Info. Division, Ext. 6782*



LBL-7284 C. 2

— LEGAL NOTICE —

This report was prepared as an account of work sponsored by the United States Government. Neither the United States nor the Department of Energy, nor any of their employees, nor any of their contractors, subcontractors, or their employees, makes any warranty, express or implied, or assumes any legal liability or responsibility for the accuracy, completeness or usefulness of any information, apparatus, product or process disclosed, or represents that its use would not infringe privately owned rights.

LBL-7284

UC-37

THE APPLICATION OF X-RAY EMISSION SPECTRA TO THE  
IDENTIFICATION OF PARTICULATE SULFUR COMPOUNDS IN AMBIENT AIR\*

A. J. Ramponi and J. M. Jaklevic

Lawrence Berkeley Laboratory  
University of California  
Berkeley, California 94720 U.S.A.

December 1978

\*Prepared for the U. S. Department of Energy  
under Contract W-7405-ENG-48



THE APPLICATION OF X-RAY EMISSION SPECTRA TO THE  
IDENTIFICATION OF PARTICULATE SULFUR COMPOUNDS IN AMBIENT AIR\*

A. J. RAMPONI AND J. M. JAKLEVIC

Lawrence Berkeley Laboratory  
University of California  
Berkeley, California 94720 USA

INTRODUCTION

It has long been observed that the x-ray emission spectrum for an ionized atom varies with the chemical environment of the atom (1). The number of allowable electronic transitions is related to the valence state of the central atom and reflects the nature of the molecular bonds formed with the neighboring ligands. The energies of the electron orbitals involved in the transitions are likewise perturbed. A number of spectroscopic techniques make use of these small energy shifts in order to identify the valence state of the atom (2). Previous workers have noted changes in the emission spectrum from sulfur compounds caused by such chemical shifts (3,4). In the present work, we employ high resolution x-ray emission spectroscopy to observe the changes in x-ray energies and relative intensities in an attempt to identify chemical compounds of particulate sulfur found in ambient air which are of interest in environmental monitoring.

A Bragg spectrometer was used to examine the sulfur  $K\alpha_{1,2}$  and  $K\beta$  regions for various sulfur-oxygen anions with the intent of measuring observable differences in the individual spectra as a function of the oxidation state of the central sulfur atom. Variations in relative intensities of the characteristic spectra were noted and the energy shifts of the peaks were measured by a least squares fitting procedure.

---

\*This work was supported by the Division of Biomedical and Environmental Research of the Department of Energy under Contract No. W-7405-ENG-48.

## EXPERIMENT

A horizontal 2 $\theta$  goniometer was used in conjunction with a stepping motor for precise incremental scanning. The stepping motor was advanced in 0.04 $^\circ$  per step and the counting period per point was chosen such that approximately 2.0-2.5 x 10 $^4$  counts would be collected at the SK $\alpha_{1,2}$  peak. The scan range was typically two degrees centered about the K $\alpha_{1,2}$  or K $\beta$  lines of sulfur. The samples were fluoresced with Cr K $\alpha$  radiation at a power of 450 W, 30 kV at 15 mA. A flat Ge <111> crystal (2d = 6.532  $\text{\AA}$ ) diffracted the sulfur x-rays into 0.005" x 3.5" Söller slits before entering a xenon gas filled proportional counter biased at 1600 V. A helium atmosphere was maintained over the entire x-ray path in order to reduce absorption of the 2.308 keV x-rays. A measured resolution (FWHM) of 3.88 eV was obtained for the K $\alpha_{1,2}$  line. A schematic diagram of the apparatus is shown in Figure 1. The proportional counter output was amplified and a single channel analyzer was used to select the SK $\alpha_{1,2}$  peak. The spectra were accumulated in a multichannel analyzer operated in a multiscaler mode synchronous with the goniometer advance.

The samples were commercial reagent grade compounds. Particle size effects were reduced by grinding to a fine powder before pressing into 1.5 mm thick disks using a 1" diameter die together with a hydraulic press (10 $^4$  psi). The resultant pellets were infinitely thick relative to the incident radiation and of uniform density.

## RESULTS AND DISCUSSION

### A) K $\alpha_{1,2}$ Emission Spectra

Although the K $\alpha_{1,2}$  line shifts observed with respect to elemental sulfur are small, they nevertheless provide some information concerning the influence that the surrounding ligands have on the central sulfur atom. Figure 2 shows the K $\alpha_{1,2}$  region for elemental sulfur which is representative of the other samples studied. The broad, high-energy bump visible at 2.322 keV can be attributed to the unresolved SK $\alpha_3$

and  $SK\alpha_4$  emission lines (5). Table 1 lists the  $K\alpha_{1,2}$  line shifts measured relative to sulfur for the compounds scanned. The measurements were performed by manually positioning the detector at the calculated  $2\theta$  setting for the  $K\alpha_{1,2}$  line of sulfur ( $E = 2.308$  keV) and then adjusting the crystal mount for maximum intensity. The other samples were then scanned without further adjustment of the apparatus. A least squares peak fitting analysis was performed on each spectrum using a Gaussian peak shape allowing for exponential tails when necessary. A linear background was constrained to pass through the endpoints of the fitting interval. Final values of the peak centroid, peak area, and the full width at half maximum of the Gaussian component of the peak and their respective uncertainties were also calculated. The shifts listed in Table 1 were determined by comparing the centroids obtained for each  $K\alpha_{1,2}$  spectrum while performing the fit. Of particular interest is the shift listed for thiosulfate,  $S_2O_3^{=}$  which contains one sulfur atom of oxidation state +6 and the other of oxidation state -2. The measured value is consistent with the fact that the  $K\alpha_{1,2}$  line shift should be a linear superposition of the sulfate (+6) and sulfide (-2) lines.

The observed shifts in inner-core binding energy arise from changes in effective charges and potentials caused by the formation of the molecular bonds. Approximate Self-Consistent Field Molecular Orbital (SCFMO) calculations using Hartree-Fock (HF) atomic wave functions have been performed by Manne (6) for most of the samples appearing in Table 1. If one assumes that the  $K\alpha_{1,2}$  ( $2p\ 1/2, 3/2 \rightarrow 1s$ ) transition\* occurs rapidly enough so that the remaining electrons do not have time to readjust (frozen-core approximation), then the same valence orbital configuration can be used before and after ionization. The energy of the  $K\alpha_{1,2}$  line is simply the energy difference between the 2p (ignoring L-S coupling) and the 1s orbital energies. Comparing this value with that obtained for elemental sulfur predicts the  $K\alpha_{1,2}$  line shift. The shifts calculated by Manne under these simplifying assumptions are

---

\*For dipole transitions the  $A_s \rightarrow B_s$  ( $A > B$ ) transition is forbidden since  $\Delta l \neq \pm 1$ .

reported in Table 1 for comparison with experiment. The agreement is surprisingly good except for sulfate which has a calculated shift that is much too large.

#### B) K $\beta$ Emission Spectra

Sulfur, being a third period element, has a ground state electron configuration resembling neon with six outer electrons (Ne)  $3s^23p^4$ . The energy level diagram for sulfur including x-ray transitions is shown in Figure 3. The K $\beta$  emission line(s) for sulfur are particularly sensitive to the chemical environment since the M-shell electrons are directly involved in the formation of the molecular orbitals with the neighboring ligands. Figure 4 shows the SK $\beta$  regions obtained from the five samples. Differences in spectra as a function of oxidation state are evident. Table 2 lists the observed peaks in each spectrum along with their respective  $K\alpha_{1,2}/K\beta$  ratios obtained by using the integrated area under the full-width at half maximum after background subtraction. The K $\beta$  line shifts measured relative to sulfur are also presented. The total shift in peak position for the compounds studied spans 1.18 eV. All shifts are to lower energies except for sulfate which shows a small positive shift. The peak shifts are consistent with the degree of valence orbital mixing which is a minimum for sulfide and a maximum for sulfate. The K $\beta$  peak width measured at half maximum differs by as much as 1.98 eV among the samples.

In an attempt to understand the diversity of the K $\beta$  spectra, molecular orbital calculations were compared with the experimental results obtained for  $SO_4^{2-}$ . Connor et al (7) have calculated the electronic structure of sulfate using all electron *ab initio* SCFMO methods. They also measured the ionization energies of the valence electrons by x-ray photoelectron spectroscopy (PES) for subsequent orbital assignment to the spectrum. The tetrahedral structure of sulfate with identical ligands surrounding the central atom implies  $T_d$  molecular symmetry. Allowed dipole transitions to the sulfur 1s level are from valence orbitals with  $t_2$  symmetry. Their results yielded three distinct bonding groups with each group consisting of 2 or 3 valence orbitals. The first

or highest energy group containing three valence orbitals is for the most part non-bonding. The second group consists of two valence orbitals. The  $4t_2$  orbital shows a high degree of mixing between the sulfur 3p and the oxygen 2p atomic orbitals. Its strong 3p character accounts for the transitions to the 1s hole giving rise to the major peak in the  $K\beta$  spectrum (Figure 4(e)). The final group of bonds also consists of two orbitals. The  $3t_2$  orbital is mostly of oxygen 2s character with some central atom 3p component. Thus, the low intensity peak appearing in the spectrum is due to transitions originating from the  $3t_2$  orbital, the observed intensity being related to the degree of occupancy by the sulfur 3p electrons in the valence orbital. Furthermore, the observed separation of  $14.04 \pm 0.09$  eV for these two lines agrees with Connor's separation of 14.1 eV as measured by PES, confirming his valence orbital assignment of these two peaks.

#### APPLICATION

A particularly interesting application to the observed spectral differences is in the identification of sulfur compounds contained in ambient aerosol particulates. Aerosol sulfur is a secondary pollutant originating from its precursor  $SO_2$ , consisting chiefly as compounds of sulfate in chemical form. A mean aerodynamic diameter of  $\sim 0.3 \mu\text{m}$  (8) makes these aerosols highly respirable and thus present a hazard to human health.

Ambient aerosols have been collected using the Automated Dichotomous Air Samplers (ADAS) (9). The air samplers were designed to simultaneously collect particulates of two different sizes by using a two-stage virtual impactor with the particle cutoff being about  $2.4 \mu\text{m}$ . The fine and coarse particles are deposited separately on 37 mm diameter filters consisting of a  $4.5 \text{ mg/cm}^2$  cellulose substrate with  $1.2 \mu\text{m}$  pore size. Elemental concentrations are determined by x-ray fluorescence (XRF) techniques. An ambient air particulate sample obtained from the smaller size fraction with a total sulfur concentration measured to be  $16.4 \pm 0.3 \mu\text{g/cm}^2$  was selected for analysis. Figure 5 shows the  $K\beta$  spectrum for

particulate sulfur in ambient air. The similarity to Figure 4(e) suggests the presence of sulfate on the filter. A comparison of spectral characteristics appears in Table 3. The results yield strong evidence for the identification of sulfate as the major component in aerosol sulfur. The absence of the side lobe on the high energy side of the main peak precludes any suggestion that sulfite,  $\text{SO}_3^-$  might be present. The intensity of the  $K\beta'$  peak and the observed peak positions is inconsistent with the presence of thiosulfate,  $\text{S}_2\text{O}_3^-$  and sulfide  $\text{S}^-$ , respectively.

The minimum detectable limits measured for the two transitions observed in the  $K\beta$  spectrum for the air pollution filter are given in Table 4. Assuming an ambient particulate sulfur concentration of  $1 \mu\text{g}/\text{m}^3$  and an air sampling rate of 50 liters/min., one would require a twelve hour sampling period for reliable sulfate analysis. Atmospheric monitoring stations typically sample for 12 or 24 hour periods and the particulate sulfur concentration is generally much higher than  $1 \mu\text{g}/\text{m}^3$  for metropolitan areas (10). As a result, the sensitivities reported in Table 4 are sufficient for making the application of this technique to sulfate measurements feasible.

### CONCLUSION

The study of x-ray emission spectra was shown to be an effective method for the observation of the chemical form of particulate sulfur in ambient air. Realizing the unique spectral characteristics of sulfate, an instrument for analyzing pollution filters for sulfate concentrations can be considered. A knowledge of the peak positions and relative peak intensities dispenses with the need to perform time consuming scans. A sealed, helium filled Bragg spectrometer that allows for precise external rotation of the diffracting crystal would permit consecutive measurements of the peak counting rates. A detailed investigation of the  $K\beta/K\beta'$  ratio (observed to be about 3 to 1) through a least squares comparison with a standard sulfate sample would yield information concerning the sulfate

concentration. Any counts remaining in the main peak after removing the sulfate contribution can be attributed to other forms of sulfur, most notably sulfides.

#### ACKNOWLEDGEMENTS

The authors wish to express their gratitude to N. Madden and W. Searles for their technical expertise and R. Gatti and R. Giaque for their assistance in the preparation of the samples investigated. Also, special thanks must go to C. Michael Lederer who furnished the peak fitting routines to perform the analysis.

REFERENCES

- 1) Azaroff, L.V., Ed., "X-Ray Spectroscopy," McGraw-Hill (1974) Chap. 9.
- 2) Herglotz, H.K. and Birks, L.S., Eds., "X-Ray Spectrometry," Marcel Dekker Inc., (1978) New York., Chap. 1.
- 3) Dzubay, T.G., Ed., "X-Ray Fluorescence Analysis of Environmental Samples," Ann Arbor Science (1977) Chap. 4.
- 4) Hurley, R.G and White, E.W., "New Soft X-Ray Method for Determining the Chemical Forms of Sulfur in Coal," Anal. Chem. 46 (1974) 2234.
- 5) Johnson, G.G. and White, E.W., "X-Ray Emission Wavelengths and keV Tables for Non-Diffractive Analysis," ASTM Data Series DS46 (1970).
- 6) Manne, R., "Molecular Orbitals and Inner-Electron-Shell Chemical Shifts for Sulfur and Chlorine Oxy-anions," J. Chem. Phys. 46 (1966) 4645.
- 7) Connor, J.A., Hiller, I.H., Saunders, V.R. and Barber, M., "On the Bonding of the Ions  $PO_4^{3-}$ ,  $SO_4^{2-}$ ,  $ClO_4^-$ ,  $ClO_3^-$  and  $CO_3^{2-}$  As Studied by X-Ray Spectroscopy and *ab initio* SCF-MO Calculations," Mol. Phys. 23 (1972) 81.
- 8) Lundgren, D.A., "Atmospheric Aerosol Composition and Concentration as a Function of Particle Size and of Time," J. Air Pollut. Contr. Ass., 20 (1970) 603.
- 9) Loo, B.W., Jaklevic, J.M. and Goulding, F.S., "Dichotomous Virtual Impactors for Large-Scale Monitoring of Airborne Particulate Matter," (1975) LBL-3854.
- 10) Loo, B.W., French, W.R., Gatti, R.C., Goulding, F.S., Jaklevic, J.M., Llacer, J. and Thompson, A.C., "Large-Scale Measurement of Airborne Particulate Sulfur," (1977) LBL-6171.

SAMPLE	FORMAL OXIDATION STATE OF SULFUR	$K_{\alpha_{1,2}}$ LINE SHIFT (eV)	
		Exptl.	Calc. <sup>a)</sup>
S	0	—	—
Cds	-2	$0.16 \pm 0.02$	—
$\text{Na}_2\text{S}_2\text{O}_3$	$\left. \begin{array}{c} -2 \\ +6 \end{array} \right\}$	$0.79 \pm 0.02$	0.9
$\text{Na}_2\text{SO}_3$	+4	$1.14 \pm 0.01$	1.2
$\text{ZnSO}_4$	+6	$1.54 \pm 0.01$	2.3

a) Reference 6.

TABLE 1. Experimental and calculated  $K_{\alpha_{1,2}}$  energy shifts relative to elemental sulfur.

SAMPLE	PEAK POSITIONS (eV)			K $\beta$ LINE SHIFT (eV)	K $\alpha_{1,2}$ /K $\beta$ RATIO
	K $\beta$	K $\beta$	K $\beta$		
S	2467.51 $\pm$ 0.09 <sup>a)</sup>	-----	-----	-----	19.1 $\pm$ 0.2
Cds	2466.59 $\pm$ 0.05	-----	-----	-0.9 $\pm$ 0.1	14.0 $\pm$ 0.2
Na <sub>2</sub> S <sub>2</sub> O <sub>3</sub>	2467.12 $\pm$ 0.04	2454.20 $\pm$ 0.18	-----	-0.39 $\pm$ 0.09	21.2 $\pm$ 0.3
Na <sub>2</sub> SO <sub>3</sub>	2466.62 $\pm$ 0.04	2451.97 $\pm$ 0.17	2472.15 $\pm$ 0.07	-0.89 $\pm$ 0.09	28.1 $\pm$ 0.4
ZnSO <sub>4</sub>	2467.79 $\pm$ 0.02	2453.74 $\pm$ 0.09	-----	+0.28 $\pm$ 0.09	27.3 $\pm$ 0.4

a) The large error is due to the greater peak width.

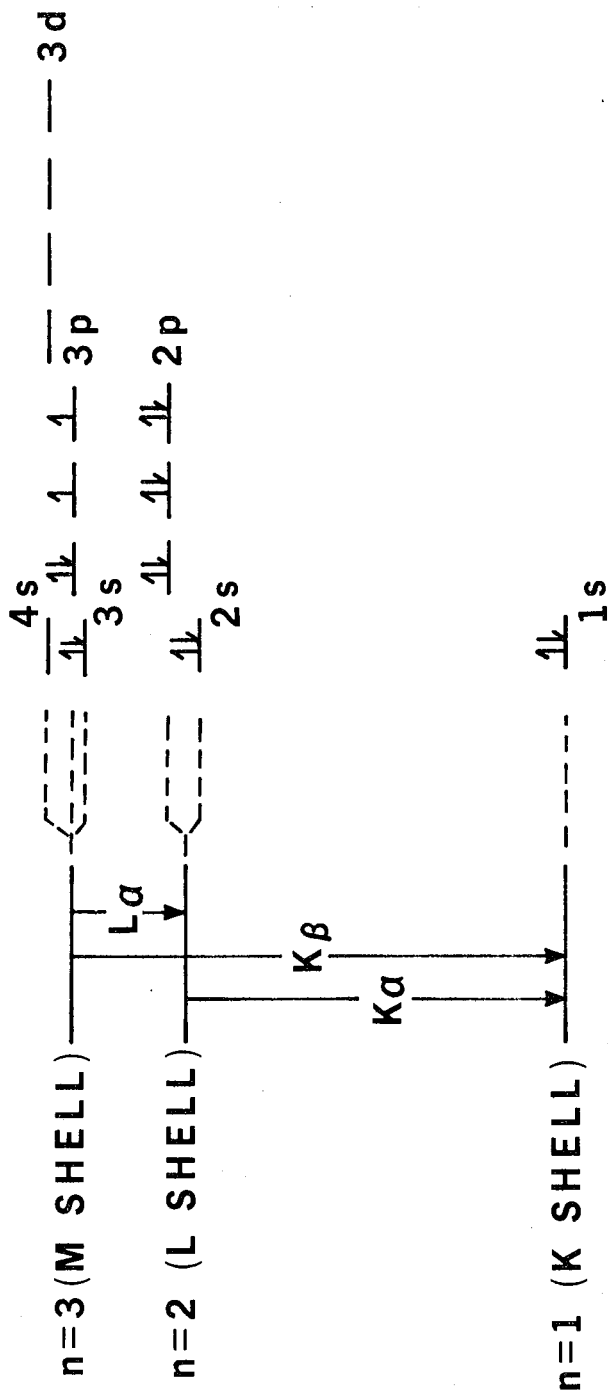
TABLE 2. K $\beta$  spectra peak positions, K $\beta$  line shifts relative to elemental sulfur, and the K $\alpha_{1,2}$ /K $\beta$  ratio for the five samples investigated.

	$K_{\alpha_{1,2}}$ LINE SHIFT (eV)	$K_{\beta}$ PEAK POSITIONS (eV)		$K_{\beta}$ LINE SHIFT (eV)	$K_{\alpha_{1,2}}/K_{\beta}$ RATIO
		$K_{\beta}$	$K_{\beta'}$		
AMBIENT SULFUR	$1.42 \pm 0.01$	$2467.82 \pm 0.05$	$2453.31 \pm 0.13$	$+0.32 \pm 0.16$	$28.0 \pm 0.05$
ZnSO <sub>4</sub>	$1.54 \pm 0.01$	$2467.79 \pm 0.02$	$2453.74 \pm 0.09$	$+0.28 \pm 0.09$	$27.3 \pm 0.4$

TABLE 3. Comparison between  $K_{\alpha_{1,2}}$  line shifts and  $K_{\beta}$  spectral characteristics for particulate sulfur in ambient air and sulfate.

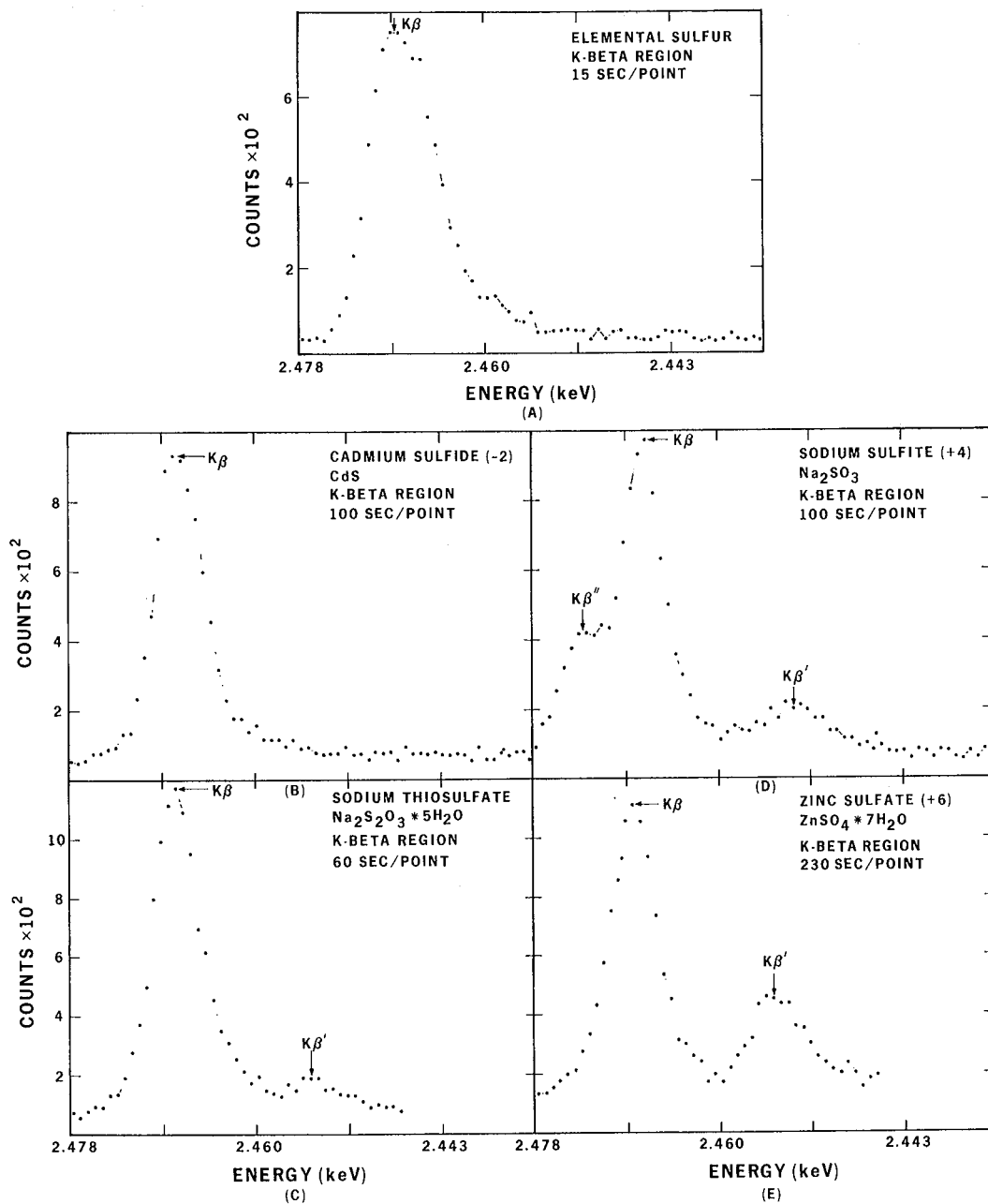
	$S \left( \frac{\text{cps}}{\mu\text{g}/\text{cm}^2} \right)$	MDL $\left( \frac{\mu\text{gm}}{\text{cm}^2} \right)$
$K_{\beta}$	0.079	1.13
$K_{\beta'}$	0.030	2.98

TABLE 4. Sensitivities and minimum detectable limits in He for the  $K_{\beta}$  spectrum of particulate sulfur present in ambient air. 500 sec counting time for 450 watts, 30 kV at 15 mA.



XBL 783-7797

Fig. 3. Energy level diagram with component subshells and x-ray transitions for sulfur. Electron filling with appropriate spin is depicted by arrows.



XBL 783-7801

Fig. 4.  $K\beta$  regions for sulfur compounds.

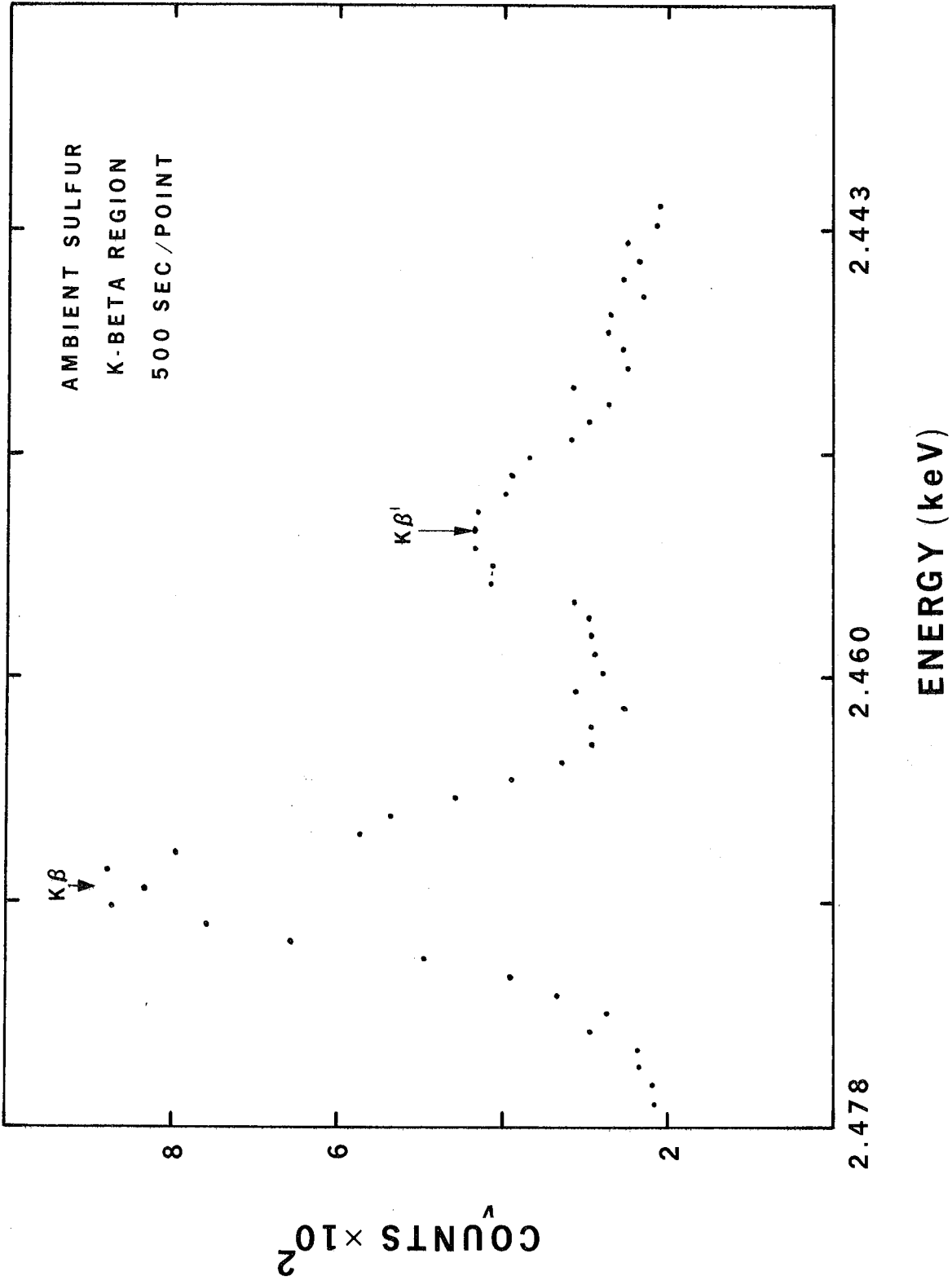


Fig. 5. Kβ region for particulate sulfur in ambient air.

XBL 783-7798

This report was done with support from the Department of Energy. Any conclusions or opinions expressed in this report represent solely those of the author(s) and not necessarily those of The Regents of the University of California, the Lawrence Berkeley Laboratory or the Department of Energy.

Reference to a company or product name does not imply approval or recommendation of the product by the University of California or the U.S. Department of Energy to the exclusion of others that may be suitable.